Energy absorbing properties of a steel profile made of dual phase steel

Wojciech Moćko[1,*], and *Adam* Brodecki[1]

[1]Motor Transport Institute, Jagiellońska 80, 03-301, Warsaw, Poland

Abstract. Three point bending tests were carried out using a drop tower testing machine. Profile were made of 2 mm dual phase steel. Material was characterized at wide range of strain rates to calibrate Rusinek-Klepaczko constitutive model. Finally, experimental results were compared with numerical predictions obtained using finite element method.

1 Introduction

Modern, advanced high-strength steels (AHSS) are – due to their high strength, ductility, strain hardening, and formability – often used in the automotive industry. The use of high-strength steel allows the reduction of the weight of energy absorbing and protective elements while maintaining the required level of vehicle passengers' protection. One of the widely used types of AHSS is Dual-Phase steels (DP). DP steel microstructure incorporates hard martensitic or bainitic phase dispersed in a soft ferritic matrix. This composition results in very good strength, drawability and work hardening. Moreover, due to good strain redistribution capacity, finished parts made of dual phase steel have superior mechanical properties to those made of as-received material. Given their high energy absorption capacity and fatigue strength, cold rolled dual phase steel is particularly well suited for automotive structural and safety parts such as longitudinal beams, cross members and reinforcements.

2 Methodology

2.1 Three point bending

The three point bending tests were carried out using the drop weight tower. The testing stand was equipped with force encoder, velocity measurement system and impact loading device. Measurement data were acquired by analog to digital converter at sampling rate equal to 1.17 MHz. Test specimens were placed on two supports constrained to the drop tower body. Distance between supports was equal to 140 mm. The impactor hits specimen in the middle of its length. Two loading cases, at two initial velocities, were considered, i.e. 11.7 m/s and 6.7 m/s. To maintain constant impact energy, equal to 600 J, the mass constrained to the impactor was adjusted.

Test specimens were fabricated from a dual phase steel of 2 mm thickness. Samples were made using sheet bending device. View of the geometry and profile of the specimens are shown in Fig. 1 and Fig. 2.

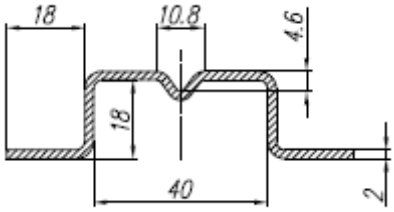

Fig. 1. Cross-section of the tests specimen applied in the three point bending test.

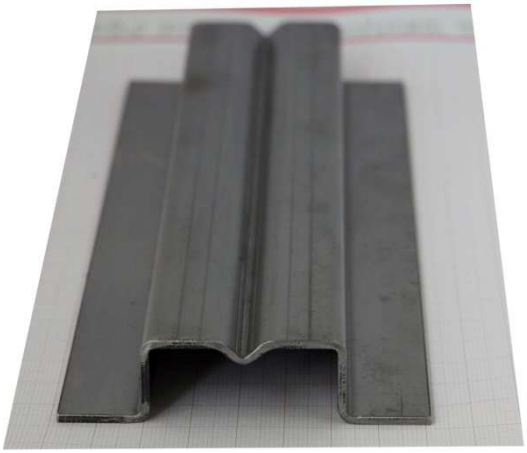

Fig. 2. View of the tests specimen in the as-received state.

2.2 Constitutive modelling

The overall flow stress in Rusinek-Klepaczko model was decomposed into three stress components: the internal stress $\bar{\sigma}_\mu(\bar{\varepsilon}^p, \dot{\varepsilon}^p, T)$, the effective stress $\bar{\sigma}^*(\dot{\varepsilon}^p, T)$ and the drag stress $\bar{\sigma}_d(\dot{\varepsilon}^p)$, as shown in Eq. 1 [1].

* Corresponding author: wojciech.mocko@its.waw.pl

$$\bar{\sigma}(\bar{\varepsilon}^p, \dot{\varepsilon}^p, T) = \frac{E(T)}{E}\left[\bar{\sigma}_\mu(\bar{\varepsilon}^p, \dot{\varepsilon}^p, T) + \bar{\sigma}^*(\dot{\varepsilon}^p, T)\right] + \bar{\sigma}_a(\dot{\varepsilon}^p) \quad (1)$$

Tensile tests were carried out using the electro-mechanical testing machine Instron E10000 and the pre-tension Hopkinson bar [2,-3] at quasi-static and dynamic range of strain rates. The testing stand at the Motor Transport Institute comes with bars 20 mm in diameter made of 7075-T6 aluminum alloy. The incident bar which is 3600 mm long is divided into a pre-tension section with a length of 1600 mm and a free end. The clamp, which confines the bar during initial loading with using a hydraulic actuator, is placed between the pre-tension and the free section of the incident bar. The length of the transmission bar is 1800 mm. The history of elastic wave in the bars is determined using tensometers, which is then amplified at the broad-band bridge [4] and finally recorded by a digital oscilloscope.

To minimize possible measurement errors the following actions were done: stress equilibrium analysis, application of high grade tensometer bridges, four radially glued tensometers measurements to avoid buckling effect, calibration of the system before each series of tests, using high resolution oscilloscope for digitizing of data, maintaining stable room temperature through tests. It must be also emphasized that all tensile tests were carried out in a series. Therefore, even in the case of some measurement errors, tendencies of change of mechanical properties of material are clearly to observe since are referred to the as-received material.

2.3 Numerical simulations

Numerical simulations of the three point bending test were carried out using ABAQUS Explicit software. View of the digital model applied for the simulation purposes is shown in Fig. 3. Specimen was represented by 23601 shell surface elements of the same geometry and dimensions like in the experimental setup. Supports and impactor were simulated by analytical surfaces. Supports were constrained, whereas initial velocity was applied to the impactor containing point mass to obtain 600 J energy.

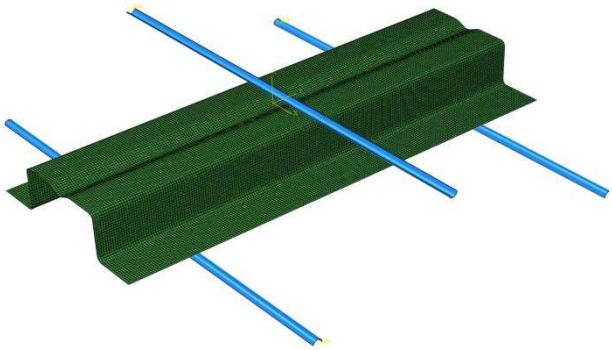

Fig. 3. Numerical model of the three point bending test.

3 Results

3.1 Calibration of the constitutive equation

Tensile tests were carried out at four various strain rates ranging from 10^{-4} s^{-1} to $6x10^{2}$ s^{-1}. Subsequently, RK equation was calibrated using obtained experimental data. Comparison of the experimental and RK model predictions of the dual phase steel is shown in Fig. 4. Constitutive equation was used to describe viscoplastic behaviour of the profiles made of dual phase steel during finite element method calculations. Methodology of true stress and true strain determining on the basis of tensile test was already shown in previous papers [5-6].

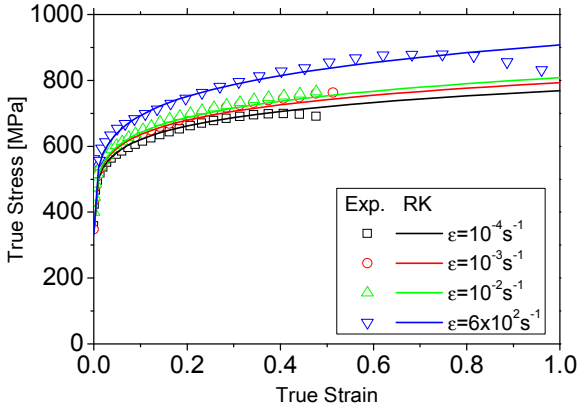

Fig. 4. Comparison of the experimental and RK model predictions of the dual phase steel.

3.2 Three point bending test

Experimental results showing mechanical behavior of the profiles made of dual phase steel are shown in Fig. 5 and Fig. 6. Histories of the impactor displacement obtained at dynamic loading experiment, at various initial velocities are shown in Fig. 5. It may be observed that displacement is not a linear function of the time, thus the velocity of the impactor is reduced due to kinetic energy dissipation during plastic deformation of the specimen.

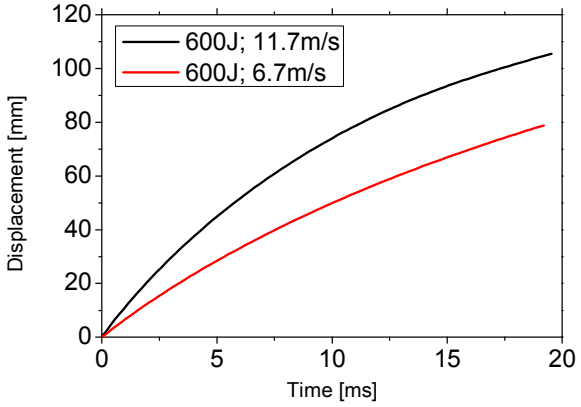

Fig. 5. Displacement of the impactor determined during dynamic three point bending test at various initial velocities.

A set of curves representing history of the force as a function of the displacement is shown in Fig. 6. The chart contains results obtained at dynamic loading conditions using drop weight tower and additionally characteristic determined at quasi-static loading conditions with the use of servo-hydraulic testing machine. It may be observed that for both loading cases there is a clearly visible maximum at displacement equal to 10 mm. At high strain rate deformation magnitude of this maximum is equal to 15 kN, whereas at low strain rates peak of the force is equal to 12 kN. At subsequent stages of deformation differences of the force history between low and high strain rate three point bending test are diminished.

Views of the specimens after three point bending test are shown in Fig. 7. It may be observed that profile is deformed mainly at central region, near place of the impactor contact with the surface of the steel.

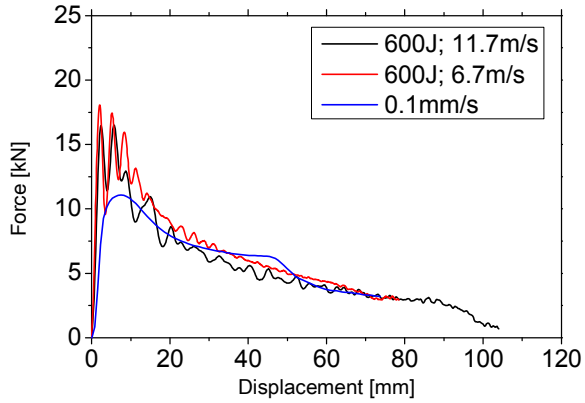

Fig. 6. History of the force vs displacement obtained during dynamic and quasi-static three point bending test.

Fig. 7. View of the specimens deformed by the three point bending test, at initial velocity 11.7 m/s.

3.3 Numerical simulation

View of the specimen exposed to three point bending tests at initial velocity equal to 11.7 m/s obtained using numerical simulations is shown in Fig. 8. The visualisation includes distribution of the von Mises stress. It may be observed that most intensive residual stress region is located in the middle of specimen near place of the impactor contact with a surface. Stress value in this area reaches 890 MPa. Other part of the specimen contains lower residual stress. Therefore it may be concluded that kinetic energy of the impactor is absorbed mainly in the central region of the specimen.

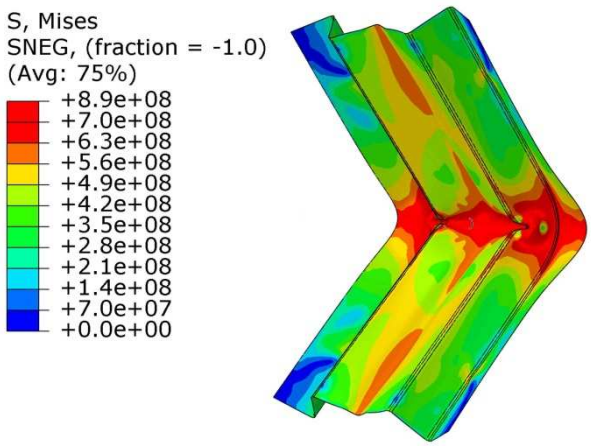

Fig. 8. Distribution of the von Mises stress calculated for the dynamic loading case at initial velocity equal to 11.7 m/s.

Comparison of the force history obtained within scope of experimental work with numerical results, at initial velocity equal to 6.7 m/s is shown in Fig. 9. It may be seen the both curves are strongly affected by oscillations at the beginning of the deformation. Maximum values are similar for experimental and numerical results, however at subsequent stages of deformation finite element method slightly underestimates value of the force.

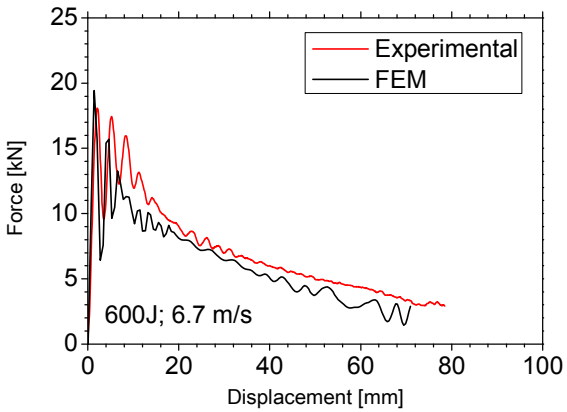

Fig. 9. Comparison between numerically and experimentally obtained history of the force vs displacement at initial velocity of the impactor equal to 6.7 m/s.

Increase of the initial velocity of the impactor induces higher magnitude of the numerically predicted oscillation at the beginning of the deformation. In the further course of specimen bending a good agreement between experimental and numerical data was obtained.

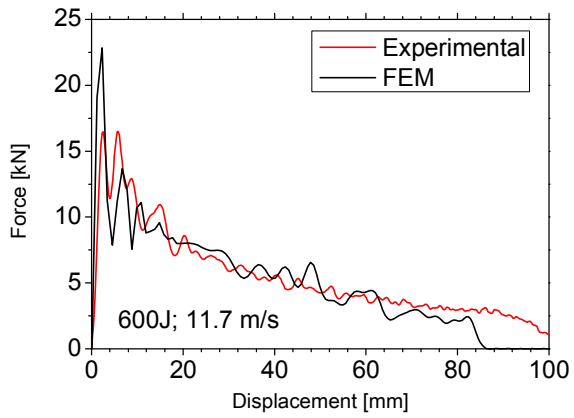

Fig. 10. Comparison between numerically and experimentally obtained history of the force vs displacement at initial velocity of the impactor equal to 11.7 m/s.

4 Summary

The goal of the analysis presented in this paper was to calibrate constitutive model and subsequently validate this model. Firstly, tensile tests were carried out to obtain mechanical characteristics of the dual phase steels. Since short specimens (5 mm width and 10 mm length of gauge) were applied during mechanical testing, therefore novel methodology of true stress and true strain estimation was employed [5-6]. This methodology is based on the use of digital image correlation to determine local strain distribution after necking point. As a consequence a set of true stress-strain curves obtained at wide range of strain rates was available. Further, family of mechanical characteristics were used to calibrate Rusinek-Klapaczko constitutive model [1]. Comparison of stress-strain charts determined experimentally and calculated using model shows good agreement, however independent method of model validation was required to confirm calibration quality. Since structures fabricated of dual phase steels are usually incorporated into vehicle chassis, therefore method of validation should be corresponding to loadings present during car crash [7].

Taking into account nature of vehicle crash and available equipment, three point bending test under dynamic loading conditions was chosen for validation purposes [8-9]. Three point bending tests were carried out using adopted drop weight tower testing stand. Dual phase sheet was formed into a profile to obtain complex stress state during plastic deformation. Experimental setup was reproduced in ABAQUS environment. Viscoplastic properties of the dual phase steel in the simulation were described by previously calibrated RK model [10]. Finally, comparison of force vs displacement curves were done to validate quality of the constitutive equation.

A good agreement between numerical and experimental data was obtained. As a consequence it may be stated that model was validated, and may be applied in vehicle crash simulation.

References

1. A. Rusinek, J.R. Klepaczko, Int. J. Plasticity, **17**, 87 (2001)
2. H. Kolsky, Proc. Phys. Soc., **62B**, 647 (1949)
3. G.H. Staab, A.A. Gilat, Exp. Mech., **31**, 232 (1991)
4. W. Moćko, Metrol. Meas. Syst., **20**, 555 (2013)
5. W. Moćko, A. Brodecki, Mater. Design, **88**, 320 (2015)
6. W. Moćko, A. Brodecki, J. Radziejewska, J. Strain Analysis, **50**, 571 (2015)
7. T.B. Hilditch, I.B. Timokhina, L.T. Robertson, E.V. Pereloma, P.D. Hodgson, Metall. Mater. Trans. A, **40**, 342 (2009)
8. J. Qin, R. Chen, X. Wen, Y. Lin, M. Liang , F. Lu, Mat. Sci. Eng. A-Struct. **586**, 62 (2013)
9. P. Baranowski, J. Janiszewski, J. Małachowski, Arch. Mech., **66**, 429-452 (2014)
10. A. Rusinek, J. A. Rodriguez-Martinez, J. R. Klepaczko, R. B. Pęcherski, Mater. Des. **30**, 1748 (2009)